Swarthmore College
Works

Physics & Astronomy Faculty Works | Physics & Astronomy

6-15-1992

Diffusion-Limited Reactions In Spherical Cavities

Amy Lisa Graves
Swarthmore College, abug1@swarthmore.edu

Elizabeth L. Grossman , '92

Dane D. Morgan III, '92

See next page for additional authors

Follow this and additional works at: https://works.swarthmore.edu/fac-physics

 Part of the Physics Commons

Let us know how access to these works benefits you

Recommended Citation

Amy Lisa Graves et al. (1992). "Diffusion-Limited Reactions In Spherical Cavities". *Journal Of Chemical Physics*. Volume 96, Issue 12. 8840-8852. DOI: 10.1063/1.462241
https://works.swarthmore.edu/fac-physics/176

This work is brought to you for free by Swarthmore College Libraries' Works. It has been accepted for inclusion in Physics & Astronomy Faculty Works by an authorized administrator of Works. For more information, please contact myworks@swarthmore.edu.

Authors

Amy Lisa Graves; Elizabeth L. Grossman , '92; Dane D. Morgan III, '92; and B. J. Berne

This article is available at Works: https://works.swarthmore.edu/fac-physics/176



Diffusion-limited reactions in spherical cavities

Amy L. R. Bug, Elizabeth L. Grossman, Dane D. Morgan III, and Bruce J. Berne

Citation: The Journal of Chemical Physics **96**, 8840 (1992); doi: 10.1063/1.462241
View online: http://dx.doi.org/10.1063/1.462241
View Table of Contents: http://scitation.aip.org/content/aip/journal/jcp/96/12?ver=pdfcov
Published by the AIP Publishing

Articles you may be interested in

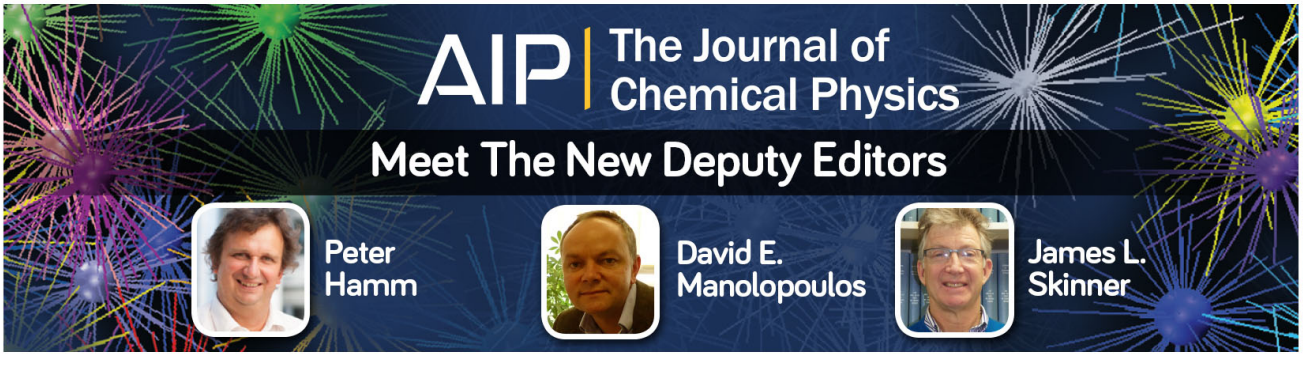
Rate of diffusion-limited reactions in a cluster of spherical sinks
J. Chem. Phys. **115**, 3827 (2001); 10.1063/1.1387978

Computer Simulations of Diffusion-Limited Reactions
Comput. Sci. Eng. **3**, 72 (2001); 10.1109/5992.895190

Diffusion-limited layer growth in spherical geometry: A numerical approach
J. Appl. Phys. **80**, 4350 (1996); 10.1063/1.363392

Rate of diffusion-limited reactions in dispersions of spherical traps via multipole scattering
J. Chem. Phys. **94**, 537 (1991); 10.1063/1.460372

On the linearized gradient approximation for diffusion-limited growth of a spherical precipitate
J. Appl. Phys. **51**, 818 (1980); 10.1063/1.327304



This article is copyrighted as indicated in the article. Reuse of AIP content is subject to the terms at: http://scitation.aip.org/termsconditions. Downloaded to IP: 130.58.65.20 On: Mon, 09 Feb 2015 20:37:43

Diffusion-limited reactions in spherical cavities

Amy L. R. Bug, Elizabeth L. Grossman, and Dane D. Morgan III
Department of Physics and Astronomy, Swarthmore College, Swarthmore, Pennsylvania 19081

Bruce J. Berne
Department of Chemistry, Columbia University, New York, New York 10027

(Received 4 October 1991; accepted 6 March 1992)

We study a quenching reaction occurring at sinks within a spherical cavity and at the cavity surface. One may think of reactions at these two, distinct locations as two, coupled reactive channels. Reactions of the type $D^* + A \rightarrow D + A$ are studied in the limit of nondilute A, present at both locations, and dilute D, present within the cavity. We use a Monte Carlo algorithm to compute mean rates, pseudo-first-order rates and branching ratios, and compare with results obtained by assuming that the two reactive channels operate in parallel. The ratio of activities of the two channels are varied; static and moving sinks are studied. We discuss an application to the determination of pore structure by NMR (nuclear magnetic resonance).

I. INTRODUCTION

It has been appreciated for many years that some bimolecular reactions are enhanced by confining one or both reagents to a restrictive geometry. The importance, for biological systems, of a diffusion space of reduced volume or dimensionality (surface diffusion) was first discussed in detail by Adam and Delbruck.[1] Micelles solvate and/or localize donors and acceptors in their interiors or on their surfaces, as in irreversible quenching reactions of the type $D^* + A \rightarrow D + A$ studied by Hatlee and co-workers.[2] In studies on reactions in the presence of surfactant aggregates[3-6] workers found the existence of new reactive channels, which typically show pseudo-first-order kinetics. Large enhancements in a reaction rate or suppression of an unwanted backreaction—useful, e.g., for the purpose of storing photochemical energy,[7,8] may also occur. On the other hand, reaction rates may be used as a probe of the shape of surfactant aggregates.[9,10] The theory of reactions in confining pores has a major application to heterogeneous catalysis; a classic work by Aris[11] relates the theory of heat and mass transport to reactions in various, realistic, pellet geometries.

A number of theoretical studies on micellar kinetic processes have appeared. Analytical solutions of the diffusion equation on or within a sphere with absorbing boundaries near the surface[12-14] or at the cavity center[1,2,15] give the rates which describe the multiple-exponential decay of concentration. Given experimental lifetimes, diffusion coefficents may be predicted.[16] Some studies[17-19] begin with rates for quenching in the micellar interior or surface, and for escape or re-entry of the donors. These studies test various models for the spatial partitioning of quenchers in, on, or near the micelles.[6] Given experimental parameters such as viscosity within micelles, bulk reaction rates, and populational parameters for micelles, these theories may predict a decay in the concentration of excited donors which is in fair agreement with experimental results.[19] If parameters of the theory are fit, agreement can be excellent.[17] Computational studies will be discussed below. In all of these modeling studies, reaction may occur at only one type of site in the system: either on sinks within a cavity, or at a cavity surface, or at a buried active site.

Here we study an irreversible, diffusion-limited, quenching reaction within a spherical cavity of micellar size. In the theoretical treatments mentioned above, competition between different reactive surfaces for reagent is not taken into account. For example, the statistics governing the distribution of sinks within the micelles are used to predict a net rate of reaction for the system. Early in the calculation, the rate for reaction in a micelle containing n sinks is assumed to be n times the rate for a micelle containing a single sink. This approximation, which holds in the dilute sink limit, treats the surface of each sink as a separate, uncoupled, reactive channel. In other words, it says that the bimolecular rate constant is independent of sink concentration. However, a concentration dependence of this rate is axiomatic within the literature on homogeneous systems of spherical sinks.[20] For example,[21] steady-state rate constants behave as $k_s[1 + \sqrt{3\phi} + \mathrm{ord}(\phi)]$ for perfectly absorbing sinks of volume fraction ϕ; k_s is the Smoluchowski[22] bimolecular rate of $4\pi Db$, with D the diffusion constant for reagent and b the sink radius. If one considers the decay, with time, of an initial concentration, the steady-state result can be equated with a mean rate of quenching with time.[23] Various studies concur that rates are around twice the Smoluchowski value for $\phi = 0.1$. Since this is a realizable concentration for many types of reactions within micelles, one should see this effect. In general, the cooperativity which occurs in an n-sink system produces a rate which exceeds n times the single-sink rate. For example, fluorescence intensities of lysopyrene quenched by pyranine at the surface of DODAC vesicles are predicted by Nomura *et al.* by assuming that quenching rates scale linearly with pyranine concentration. (This linearity is embodied in the Stern–Volmer formula.[24,25]) However, calculated intensities fall systematically below experiment (Table II of Ref. 8) as pyranine concentration increases, as we might expect.

 0021-9606/92/128840-13$06.00 © 1992 American Institute of Physics
This article is copyrighted as indicated in the article. Reuse of AIP content is subject to the terms at: http://scitation.aip.org/termsconditions. Downloaded to IP: 130.58.65.20 On: Mon, 09 Feb 2015 20:37:43

In this paper, we study the enhancement of the diffusion-limited reaction which occurs by allowing reaction to occur simultaneously at two different types of site. These are (i) at the surface of one or more sinks within the cavity volume and (ii) at the cavity surface. By "enhancement," we mean the factor by which the rate of reaction exceeds the sum of the rates that we would calculate if one of the two types of sites were rendered inert. We compute both a mean and a pseudo-first-order rate; these are defined in Sec. II below. We find that enhancements greater than 1/3 can be seen in Monte Carlo (MC) data from the quenching of donors 5.0 Å in diameter by like-sized spheres at an effective volume fraction of approximately 0.2. One implication is that, if one is interested in catalyzing such a reaction with high efficiency in a micellar system or a microporous solid, one might try to introduce acceptors (possibly, two different, accepting species) which sit at the two different locations.

The paper is organized as follows. In Sec. II, we describe the quenching reaction to be studied and the rates to be calculated. We also discuss an analytically solvable case; that of a spherical sink at the micelle center. (This case is often used as a point of reference, despite the fact that there are good reasons to assume that a mobile sink will typically *avoid* this location.[13]) In Sec. III, we digress to the case of a two-dimensional, model capillary with absorbing sinks at the walls, to observe the effect that competition between walls has on a rate constant. We discuss an application other than a chemical reaction: the use of spin–lattice relaxation times in NMR (nuclear magnetic resonance) to deduce the structure of pores within microporous solids. In Sec. IV, we present the results of MC simulations of a model micelle containing several sinks. The reaction is primarily diffusion limited, though the ratio of reactivities of sinks and the cavity wall are varied to study the important case in which the branching ratio is approximately unity. Both static and moving sinks are studied and rates are averaged over sink configurations. Our goal is to determine the enhancement of reactivity when the dispersed sinks and the cavity walls compete to absorb reagent.

II. QUENCHING REACTION IN A SPHERICAL CAVITY

Consider a spherical cavity in which a species D (donor) is free to diffuse. This molecule is modeled as a sphere; it may approach no closer than its radius to the cavity wall. It may not overlap with a second molecular species which is placed within the cavity. In a typical fluorescence quenching experiment, it is possible to insure that at most one D will be found in any spherical micelle, along with a number of molecules A, which serve as acceptors for an excitation of the donor.[5,6] Depending on the identity of A, it is also possible to find D within the cavity, but A's are located at the surface. One may have such a high concentration of A that the surface of the cavity is completely saturated.[8] We propose to model an experiment in which, at an initial time, donors are photoexcited, and may be quenched by acceptors. Schematically, $D \rightarrow D^*$ followed by $D^* + A \rightarrow D + A$. Experimentally, one follows the intensity of fluorescence that accompanies the de-excitation of D. There will, of course, be spontaneous de-excitation of D*, but this process occurs in parallel with quenching by A, so the net fluorescence rate is just a sum of the two rates.

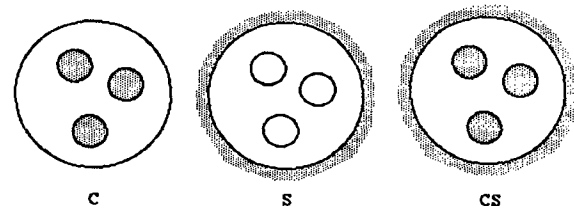


FIG. 1. Three schemes for the location of quenching surfaces within a spherical cavity. Hatched areas represent partially absorbing surfaces; unhatched areas represent reflecting surfaces. Schemes are noted as C, acceptors in center; S, at surface; and CS, at both locations. (The text discusses various numbers of spheres; for simplicity, three are shown in this figure.)

We consider a single geometry: a spherical cavity of radius R containing a certain volume fraction of spheres which are impenetrable to a single, enclosed, D molecule. Against the backdrop of this geometry, we consider three schemes for the placement of A molecules. In the first, the A molecules coincide with the spheres, making them quenchers (sinks) for the reagent, D*. In the second, quenching occurs at the surface of the cavity; the impenetrable spheres are, nevertheless, present so that we may compare situations in which D* has the same free volume in which to diffuse. In the third scheme, the A molecules coincide with the spheres *and* saturate the surface of the cavity. These will be referred to as schemes C, S, and CS, respectively, and are shown schematically, for three enclosed spheres, in Fig. 1. A given scheme determines which of the bounding surfaces merely reflect, and which quench, in the following time-dependent diffusion equation for the concentration, $C(\mathbf{r},t)$ of D* within the cavity:

$$\frac{\partial C(\mathbf{r},t)}{\partial t} = D\nabla^2 C(\mathbf{r},t) \tag{1}$$

subject to

$$\frac{\partial C(\mathbf{r}_{Q_i},t)}{\partial n} = -h_{Q_i} C(\mathbf{r}_{Q_i},t); \frac{\partial C(\mathbf{r}_N,t)}{\partial n} = 0 \ \forall t. \tag{2}$$

A development of these equations in the context of catalysis can be found in Chap. 2 of Ref. 11. In Eq. (1), D is the self-diffusion coefficient for D* within the micelle. In Eq. (2), $\mathbf{r}_{Q_i}$ and $\mathbf{r}_N$ represent any location on a quenching (we will also use the term absorbing) or reflecting surface, respectively, n is a surface normal, and h_{Q_i} describes the reactivity of the ith quenching surface. A vanishing h_{Q_i} indicates reflection, and perfect absorption implies that this number is infinite. In this case,

$$C(\mathbf{r}_{Q_i},t) = 0 \quad \text{(perfect absorber)}. \tag{3}$$

If $1/(h_{Q_i}^2 D)$ is very much less than the typical time that it takes for reagent to visit the ith surface; and in the extreme limit, if Eq. (3) holds, reaction of D* with that surface is considered to be *diffusion limited.*

This article is copyrighted as indicated in the article. Reuse of AIP content is subject to the terms at: http://scitation.aip.org/termsconditions. Downloaded to IP: 130.58.65.20 On: Mon, 09 Feb 2015 20:37:43

Assume, for now, that the bounding surfaces do not change with time. A unique solution to Eqs. (1)–(3) corresponds to a given geometry as in Fig. 1. Separation of variables: $C \equiv T(t)X(\mathbf{r})$, and solution of the resulting Helmholtz equation for X produces a series solution[15,26]

$$C(\mathbf{r},t) = \sum_n B_n X_n(\mathbf{r}) e^{-D\alpha_n^2 t}. \tag{4}$$

The eigenvalues α_n, and the associated eigenmodes X_n, depend on the boundary conditions, as given by the radii and placement of spheres, cavity radius, which case among C, S, or CS we choose, values of h_{Q_i} for absorbing surfaces, and the radius of the diffusing sphere. (The diffuser is not a point, so the bounding surfaces are not necessarily those of small spheres enclosed by a larger sphere.) The amplitudes B_n are determined by the initial concentration of D*. The X_n are orthogonal for different values of n, so that

$$B_n = \int C(\mathbf{r},0) X_n^*(\mathbf{r}) d^3r \Big/ \int X^* X \, d^3r. \tag{5}$$

Consider the likelihood, $P(t)$, that D* is present in the cavity at time t

$$P(t) = \int C(\mathbf{r},t) d^3r. \tag{6}$$

At short times, $P(t)$ receives contributions from many exponentially decaying modes. In this limit, for diffusion-limited reactions, P has alternatively been expressed as a stretched exponential.[27,28] At long times, the likelihood will decay as a single exponential, with a relaxation time of $1/k_0$ with $k_0 \equiv D\alpha_0^2$, which corresponds to the longest time scale in Eq. (4)

$$P(t) \propto e^{-k_0 t} \quad \text{as } t \to \infty. \tag{7}$$

This rate, k_0, is the *pseudo-first-order rate*. In fluorescence quenching experiments, the long time decay of fluorescence typically gives an excellent fit to a single-exponential form, allowing this constant (or an analogous one which takes into account the entry and exit of quenchers from a micelle) to be computed.[17,19]

A second rate, which is commonly used in first-passage time problems,[29] is the *mean rate*, k. This rate (which is equivalent to the rate above for a pure, single-exponential process) is defined as

$$1/k = \int_0^\infty P(t) dt. \tag{8}$$

This is the quantity that should be equated with the steady-state rate.[23] It is often used, is readily calculated for reactors with simple geometries,[6] and has been shown to be useful for solving problems in which the diffuser obeys a generalized (Smoluchowski) diffusion equation.[30]

A. Central sphere model: Pseudo-first-order rates

Consider a single molecule A, of radius a, fixed at the center of a sphere of radius R. In this geometry, we use a point walker, D*. Assume that in cases C and CS (as in Fig. 1, but now with only a single, central sphere), A is a perfect quencher, [Eq. (3)], and that in cases S and CS, the surface of the micelle quenches with a strength h_S [Eq. (2)]. Equation (1) has been well studied for this geometry, and we quote the solution[1,15] for the case of a spherically symmetric initial distribution, $C(r,0)$.

Case C:

$$C(\mathbf{r},t) = \sum_{n=0}^\infty B_n^{\mathrm{C}} \frac{\sin[\alpha_n(r-a)]}{r} e^{-D\alpha_n^2 t}, \tag{9}$$

with B_n^{C} a known function of a, R, and $C(r,0)$. It is given by Eq. (5) with $X_n(r) = j_0(\alpha_n r)$, a spherical Bessel of zeroth order. In these equations, α_n is the nth root of

$$\alpha_n(R-a)\cot\alpha_n(R-a) = \left(1 - \frac{a}{R}\right). \tag{10}$$

Two limits for k_0 given by the transcendental Eq. (10) might be noted. In the limit of a weakly quenching reactor, which is accomplished by shrinking the central sink,

$$k_0 \cong \frac{3Da}{R^3} \quad \text{for } a/R \ll 1. \tag{11}$$

In the limit where the central sink grows to fill the cavity

$$k_0 \cong \frac{D\pi^2}{4R^2(1-a/R)^2} \quad \text{for } (1-a/R) \ll 1. \tag{12}$$

Case S:

$$C(\mathbf{r},t) = \sum_{n=0}^\infty B_n^{\mathrm{S}} \frac{\sin[\alpha_n(r-a)] + a\alpha_n \cos[(r-a)\alpha_n]}{r} \times e^{-D\alpha_n^2 t}, \tag{13}$$

with B_n^{S} a known function of h_S, a, R, and $C(\mathbf{r},0)$ [Eq. (5)], and α_n given by

$$(h_S R - 1 - aR\alpha_n^2)\sin[\alpha_n(R-a)] + R\alpha_n\left[h_S a + \left(1 - \frac{a}{R}\right)\right]\cos[\alpha_n(R-a)] = 0. \tag{14}$$

Two limits for k_0: For the weakly quenching reactor, for all values of a/R so long as the central sink does not grow to fill the cavity

$$k_0 \cong \frac{3Dh_S}{3a(1-a/R) + R(1-a/R)^3} \quad \text{for } h_S R \ll 1 - a/R. \tag{15}$$

The limit in which the micellar surface becomes a strong quencher yields a simple form for k_0, if we make the additional provision that a is close (but not equal) to R

$$k_0 \cong \frac{D\pi^2}{4R^2}\left(\frac{1}{1-a/R} + \frac{4R}{\pi^2 a}\right)^2$$

so long as

$$h_S R(1-a/R)^2 \gg 1. \tag{16}$$

Equation (16) neglects terms of ord$(1/h_S R)$.

Case CS:

$$C(\mathbf{r},t) = \sum_{n=0}^\infty B_n^{\mathrm{CS}} \frac{\sin[\alpha_n(r-a)]}{r} e^{-D\alpha_n^2 t} \tag{17}$$

with B_n^{CS} a known function of h_S, a, R, and $C(\mathbf{r},0)$ [Eq. (5)], and α_n the nth root of

This article is copyrighted as indicated in the article. Reuse of AIP content is subject to the terms at: http://scitation.aip.org/termsconditions. Downloaded to IP: 130.58.65.20 On: Mon, 09 Feb 2015 20:37:43

$$\alpha_n(R-a)\cot\alpha_n(R-a)=(1-h_SR)\left(1-\frac{a}{R}\right). \tag{18}$$

In the limit of a weakly quenching reactor (accomplished by both shrinking the central sink and weakening the quenching strength of the micellar surface),

$$k_0\cong\frac{3D}{R^2}\left(h_SR+\frac{a}{R}\right)\quad\text{for } h_SR+a/R\ll 1. \tag{19}$$

In the limit in which the micellar surface becomes a strong quencher (so long as the central sink does not grow to fill the cavity)

$$k_0\cong\frac{D\pi^2}{R^2(1-a/R)^2}$$

so long as

$$h_SR(1-a/R)\gg 1. \tag{20}$$

Equation (20) neglects a term of ord$[1/(h_SR)(1-a/R)]$.

The formulas above allow us to compare the pseudo-first-order rate for scheme CS, k_0^{CS}, to the sum of the rates for schemes C and S, k_0^C and k_0^S. We define the enhancement, Δk_0, as an absolute increase in the rate

$$\Delta k_0=k_0^{CS}-(k_0^C+k_0^S); \tag{21}$$

the relative enhancement,

$$\delta k_0=\Delta k_0/k_0^{CS} \tag{22}$$

is also of interest. The task is just to solve the transcendental Eqs. (10), (14), and (18) as the dimensionless parameters h_SR and a/R are varied. Before doing so, note that $\Delta k_0\cong 0$ in the weak quenching limits, which are described by Eqs. (11), (15), and (19). That is, to first order in h_SR and a/R, the reactive channels at the surface and center of the micelle, as measured by k_0, operate in parallel. In this limit of small h_S, the reaction at the surface is *not* diffusion, but activity limited.

As h_S grows, the enhancement grows from zero. Figures 2 show k_0's, Δk_0, and δk_0 to be monotonically increasing functions of h_s, for a given value of a. (We let $R=D=1$.) As seen in Fig. 2(a), k_0^{CS} (and k_0^S) rise with a negative curvature as h_S grows. This is sensible because in the limit of large h_S, the reaction becomes diffusion limited, so k_0^{CS} and k_0^S saturate. These saturated values are given by the limits Eqs. (16) and (20).

Δk_0 [Fig. 2(b)] and δk_0 [Fig. 2(c)] must also saturate. Something interesting appears if we consider the latter: It does not increase monotonically as the radius of the central sphere grows. (Note a crossover between various curves at low and at high h_S.) Figures 3 show rates and enhancements as a function of a for several values of h_S. Though k_0 and Δk_0 increase monotonically with a, δk_0 [Fig. 3(c)] displays a single maximum. Curves for successively larger values of h_s envelope one another, as Fig. 2(c) would predict. The maximum, $\delta k_0^{max}(h_S)$, increases in value as h_S increases, and it also falls at a larger values of $a\equiv a^{max}$. Thus for a sink of given size, there is a value of the micellar surface reactivity that will maximize the relative enhancement of the

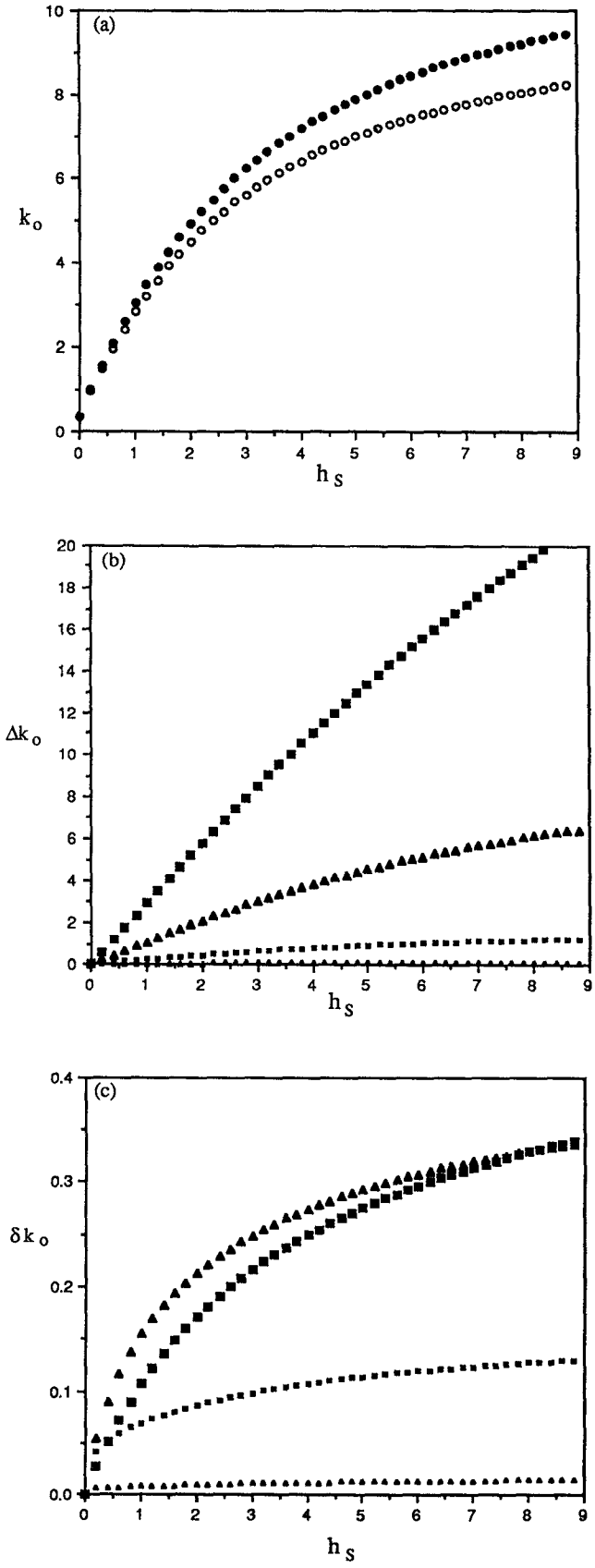


FIG. 2. (a) Pseudo-first-order rate as a function of h_S, the reactivity of the cavity surface, for central sphere radius $a=0.1$. Empty circles: $k_0^C+k_0^S$, filled circles: k_0^{CS}. (b) Absolute enhancement of k_0 vs h_S. Small triangles: $a=0.01$, small squares: $a=0.1$, large triangles: $a=0.4$, large squares: $a=0.7$. (c) Relative enhancement of k_0 vs h_S. Symbols as in (b).

This article is copyrighted as indicated in the article. Reuse of AIP content is subject to the terms at: http://scitation.aip.org/termsconditions. Downloaded to IP: 130.58.65.20 On: Mon, 09 Feb 2015 20:37:43

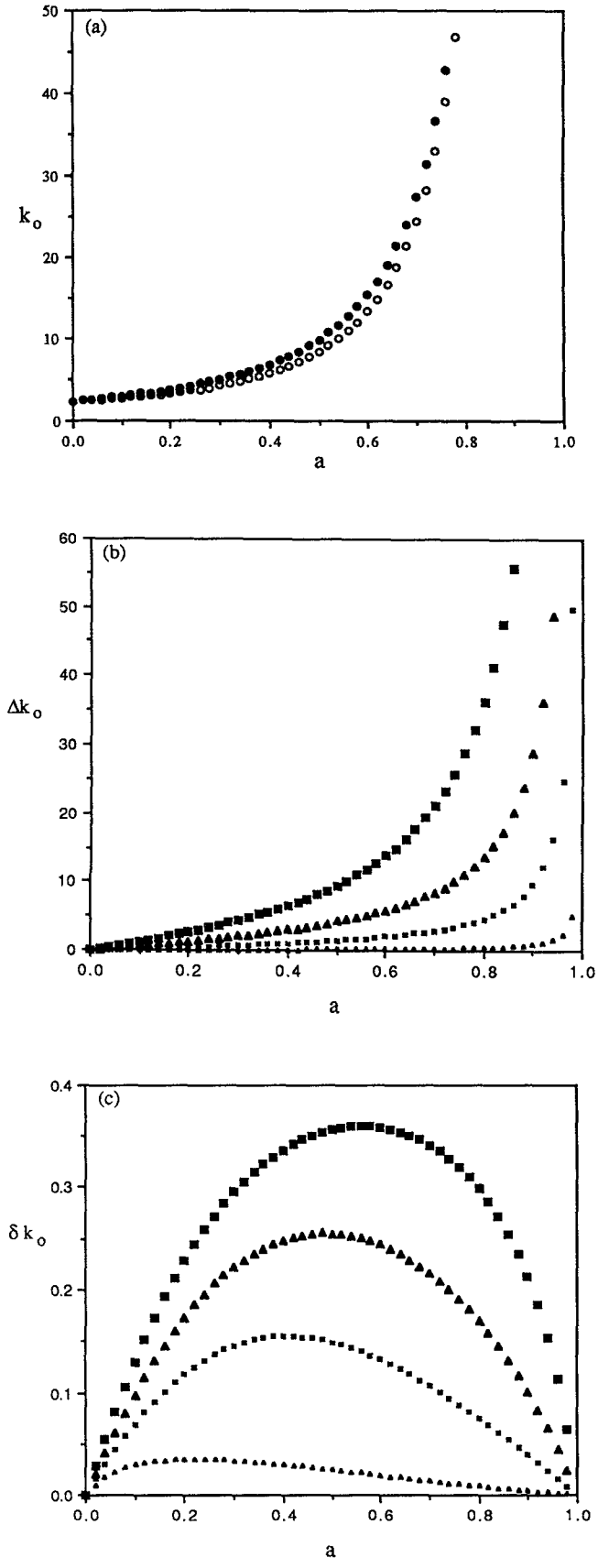


FIG. 3. (a) Pseudo-first-order rate as a function of a, for $h_S = 1$. Symbols as in Fig. 2(a). (b) Absolute enhancement of k_0 vs a. Small triangles: $h_S = 0.1$, small squares: $h_S = 1$, large triangles: $h_S = 3$, large squares: $h_S = 9$. (c) Relative enhancement of k_0 vs a. Symbols as in (b).

quenching rate. Similarly, if one is given the surface reactivity, there is a value of sink radius, $a^{\max}$ that is optimal. Below, we will note that this radius varies with the surface reactivity in a way which is correlated with the *branching ratio*.

As mentioned above, the enhancement saturates at a large-h_S limit, which is a-dependent. When $a \approx R$, the reaction rates in cases C, S, and CS, per unit surface area of the wall, will be equivalent to the rates for reaction between two infinite planar walls separated by a distance $R - a$. Equations (12), (16), and (20) confirm this for the case of very large h_S. That is,

$$k_0^{\mathrm{C}} = k_0^{\mathrm{S}} \cong \frac{D\pi^2}{4(R-a)^2};$$

$$k_0^{\mathrm{CS}} \cong \frac{D\pi^2}{(R-a)^2} \quad \text{when } h_s \to \infty, \quad a \to R. \tag{23}$$

Thus

$$\delta k_0 = \delta k_0^{\max}(h_S \cong \infty) \cong \tfrac{1}{2} \tag{24}$$

for this diffusion-limited reaction between two infinitesmally separated, spherical surfaces.

One can get some feeling for this enhancement by noting that k_0 is related to the shape of the zeroth eigenmode, X_0, and comes from a variational principle[26,31]

$$k_0 = \min \frac{\int |\nabla \psi|^2 \, d\mathbf{r}}{\int |\psi|^2 \, d\mathbf{r}} = \frac{\int |\nabla X_0|^2 \, d\mathbf{r}}{\int |X_0|^2 \, d\mathbf{r}}, \tag{25}$$

where ψ is any function that obeys Eqs. (1)–(3) and the integral is over the cavity. So, the ground state, X_0, is the solution to the correct equation, with the correct boundary conditions, which minimizes the mean squared curvature. If one takes a given geometry with a reflecting and a quenching surface, and converts both to quenchers, the mean curvature of the ground state solution rises. In the case of two planar walls and perfect quenching, it doubles. But k_0 goes as the square of the curvature, so the rate is enhanced by a factor of (1/2) [Eq. (24)] over the sum of the rates of the two, competing reactions. This is an upper limit for δk_0 for the central-sphere model. Further, one feels that it might also be an upper limit for enhancement due to competition between arbitrarily placed spheres and a cavity wall, and even for the competition between the multiple spheres in a cavity or in a homogeneous system.

One might wonder if the value of the sink radius, $a^{\max}$, at which δk_0 has its maximum, varies with h_S in a way which can be predicted by the branching ratio, B. That is, since competition between reactive surfaces produces enhancement, perhaps $a^{\max}$ occurs where $B \approx 1$. We define B as the ratio of reagent quenched by the central sink to that quenched at the surface in case CS. This ratio of reactive fluxes is

$$B = \frac{|\nabla C(a,t)|a^2}{|\nabla C(R,t)|R^2}. \tag{26}$$

To be consistent, we investigate the long time approximation, in which pseudo-first-order kinetics occurs. In this limit, B is time independent and is given by

This article is copyrighted as indicated in the article. Reuse of AIP content is subject to the terms at: http://scitation.aip.org/termsconditions. Downloaded to IP: 130.58.65.20 On: Mon, 09 Feb 2015 20:37:43

TABLE I. Branching ratios and relative enhancements at the value of a which maximizes the latter, for various values of th micellar surface reactivity.

B	$\delta k_0^{\max}$	$a^{\max}$	h_S
3.26	0.035	0.22	0.1
1.04	0.155	0.40	1.0
0.71	0.255	0.48	3.0
0.61	0.360	0.56	9.0
0.63	0.416	0.62	20.0
1.0	0.5	1.0	∞

$$B \cong \frac{a\alpha_0}{hR \sin[\alpha_0(R-a)]} \quad \text{for large } t. \tag{27}$$

Equation (27) is found by substituting the first term of the solution, Eq. (17) into the definition, Eq. (26), and applying the boundary condition, Eq. (18). One evaluates α_0, and hence Eq. (27), numerically to find that it is not true that the branching ratio, B, is precisely unity at $a^{\max}$ for arbitrary h_S. Nevertheless, it is close,

$$B \sim 1 \quad \text{for } h_S \not\ll 1. \tag{28}$$

Table I lists B and δk_0 at $a^{\max}$ for several values of h_S. B falls to roughly 0.6 before it begins to rise to its large h_S limit of 1, where $a^{\max} \approx 1$ as well. In this limit, Eq. (27) predicts that $B \approx a/R$, so that the branching ratio at $a^{\max}$ is roughly $a^{\max}/R$. The large (small) h_S limit gives large(small) enhancements (Figs. 2), so the former are the most important to us. In summary, it is not a bad rule of thumb to say that choosing a sink radius and a cavity reactivity that keep $B \approx 1$ will help one see a good relative enhancement in the rate of reaction.

B. Central sphere model: Mean rates

The mean rate, k, is defined in Eq. (8) by integrating the survival probability, $P(t)$, over time. One need not first find $C(\mathbf{r},t)$ to substitute in Eq. (6), but may instead integrate the diffusion equation, Eq. (1), over time. That is, suppose that D* begins at location r and is eventually quenched, so that if $W(\mathbf{r},t)$ is the probability of seeing D* within a small volume centered on r, W obeys the diffusion equation with temporal boundary conditions

$$W(\mathbf{r},t=0)=1 \quad \text{and} \quad W(\mathbf{r},\infty)=0. \tag{29}$$

Then the reaction time, $\tau(\mathbf{r})$, which is defined as[6,16,30]

$$\tau(\mathbf{r}) = \int_0^\infty W(\mathbf{r},t)dt, \tag{30}$$

obeys

$$D\nabla^2\tau(\mathbf{r}) = -1. \tag{31}$$

The mean reaction time, $\bar{\tau}$, is $\tau(\mathbf{r})$ averaged over all initial positions; the mean rate of Eq. (8) is its inverse

$$\bar{\tau} \equiv 1/k = \int \rho(\mathbf{r})\tau(\mathbf{r})d\mathbf{r}. \tag{32}$$

The density $\rho(\mathbf{r})$ describes the probable position of D* at $t=0$.

From here on, we assume that τ and ρ are spherically symmetric. Equation (31) is solved subject to boundary conditions on $\tau(r)$. For the present study, these come directly from Eq. (2) and are

$$\text{Case C: } \tau(a)=0; \quad \frac{\partial\tau(R)}{\partial r}=0, \tag{33}$$

$$\text{Case S: } \frac{\partial\tau(a)}{\partial r}=0; \quad \frac{\partial\tau(R)}{\partial r}=-h_S\tau(R), \tag{34}$$

$$\text{Case CS: } \tau(a)=0; \quad \frac{\partial\tau(R)}{\partial r}=-h_S\tau(R). \tag{35}$$

The general solution to Eq. (31) is a sum of a homogeneous and a particular solution

$$\tau(r) = A/r + B + r^2/6D. \tag{36}$$

The constants in the homogeneous solution, A and B, are determined by the boundary conditions, Eqs. (33)–(35); the mean reaction rate is then determined by the integral, Eq. (32). If we assume that the initial concentration, $\rho(r)$ is uniform within the cavity outside of the central sphere, and zero within it, so that

$$1/k = \frac{3}{R^3-a^3}\int_a^R r^2[A/r + B + Cr^2]dr, \tag{37}$$

then the solutions of Eq. (37) for schemes C, S, and CS are straightforward;

$$\text{Case C: } k^{\mathrm{C}} = \frac{15Da(R^2+Ra+a^2)}{(R-a)^2[5R^3+6R^2a+3Ra^2+a^3]}, \tag{38}$$

$$\text{Case S: } k^{\mathrm{S}} = \frac{15Dh_SR^2(R^2+Ra+a^2)}{(R-a)[5R^4+10R^3a+15R^2a^2+10Ra^3+5a^4+h_S(R^5+2R^4a+3R^3a^2-R^2a^3-5Ra^4)]}, \tag{39}$$

$$\text{Case CS: } k^{\mathrm{CS}} = \frac{60D(R^2+Ra+a^2)(h_SR^2-h_SRa+a)}{(R-a)^2[20R^3+24R^2a+12Ra^2+4a^3+h_S(4R^4+3R^3a-3R^2a^2-4Ra^3)]}. \tag{40}$$

Our purpose is to find reactive enhancements, the absolute

$$\Delta k = k^{\mathrm{CS}} - (k^{\mathrm{C}} + k^{\mathrm{S}}), \tag{41}$$

and the relative

$$\delta k = \Delta k / k^{\mathrm{CS}}, \tag{42}$$

which are the analogs of Eqs. (21) and (22) for the pseudo-first-order rates. These are shown in Figs. 4 and 5. These figures are qualitatively similar to Figs. 2 and 3, though the

This article is copyrighted as indicated in the article. Reuse of AIP content is subject to the terms at: http://scitation.aip.org/termsconditions. Downloaded to IP: 130.58.65.20 On: Mon, 09 Feb 2015 20:37:43

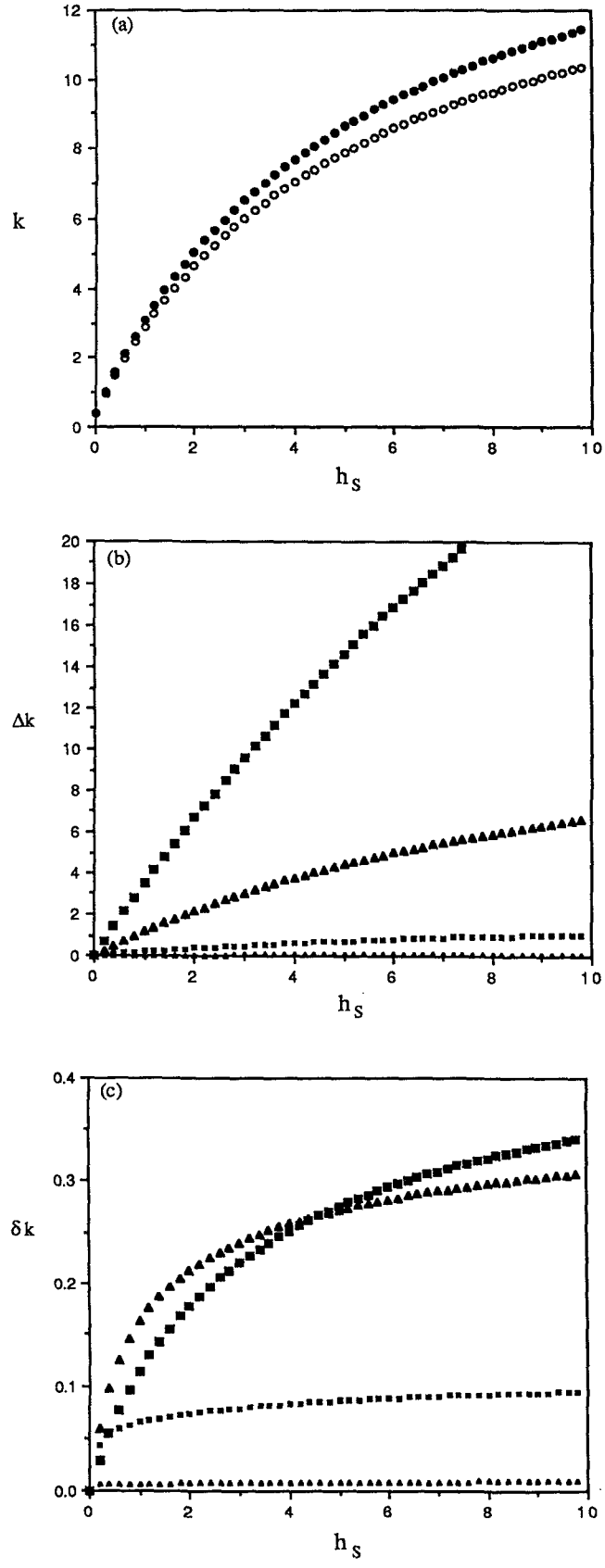


FIG. 4. (a) Mean rate as a function of h_S; central sphere has radius $a = 0.1$. Empty circles: $k^C + k^S$, filled circles: k^{CS}. (b) Absolute enhancement of k vs h_S. Small triangles: $a = 0.01$, small squares: $a = 0.1$, large triangles: $a = 0.4$, large squares: $a = 0.7$. (c) Relative enhancement of k vs h_S. Symbols as in (b).

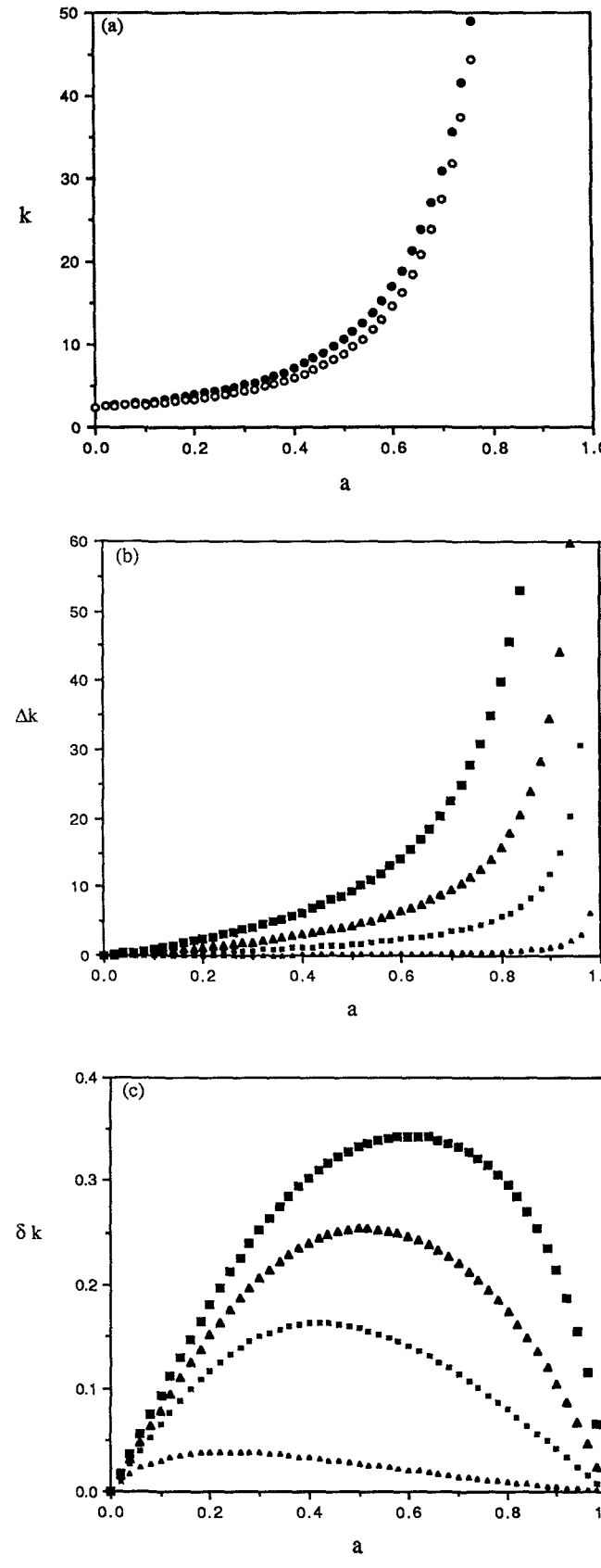


FIG. 5. (a) Mean rate as a function of a, for $h_S = 1$. Symbols as in Fig. 4(a). (b) Absolute enhancement of k vs a. Small triangles: $h_S = 0.1$, small squares: $h_S = 1$, large triangles: $h_S = 3$, large squares: $h_S = 9$. (c) Relative enhancement of k vs a. Symbols as in (b).

This article is copyrighted as indicated in the article. Reuse of AIP content is subject to the terms at: http://scitation.aip.org/termsconditions. Downloaded to IP: 130.58.65.20 On: Mon, 09 Feb 2015 20:37:43

mean rate, k, exceeds k_0 for given values of a and h_S. One sees competition between sinks [Figs. 4(a) and 5(a)] and absolute enhancements that grow with h_S and a [Figs. 4(b) and 5(b)]. One also sees a peak value, $\delta k^{\max}$ of the relative enhancement [Fig. 5(c)] at an intermediate sink radius, $a^{\max}$. There is scant quantitative difference between $\delta k^{\max}$ and $\delta k_0^{\max}$ for a given h_S; the values, $a^{\max}$, at which these peaks occur are similar as well. In short, the mean and psuedo-first-order rates provide similar evidence of reactive enhancement due to competition between the central sink and micellar surface.

III. APPLICATION TO NMR DETERMINATION OF PORE STRUCTURE

NMR is an important tool in the determination of the structure of porous solids.[32] For example, ^{129}Xe within the pore spaces of a zeolite may produce a signal with peaks of different strengths centered at different chemical shifts. These strengths give one an estimate of the distribution of pore sizes in the solid.[33] As an alternative to looking at chemical shifts, pore structure can be inferred by following the dynamics of spins within the pores as they evolve in time. The typical time for an initially aligned population of nuclei to disalign due to collisions with the walls is called T_1, a spin–lattice relaxation time.

One can write an expression for the time evolution of the magnetization, $m(\mathbf{r},t)$, which models the motion of the nuclei as diffusive, and assumes that m decays at a fixed rate in the bulk. This decay occurs at a different rate if $\mathbf{r}$ is $\mathbf{r}_{Q_i}$, a location on the ith region of pore wall. In other words,[34,35]

$$\frac{\partial m(\mathbf{r},t)}{\partial t} = D\nabla^2 m(\mathbf{r},t) - k_B m(\mathbf{r},t) \tag{43}$$

subject to

$$\frac{\partial m(\mathbf{r}_{Q_i},t)}{\partial n} = -h_{Q_i} m(\mathbf{r}_{Q_i},t) \forall t. \tag{44}$$

The analogy to Eqs. (1) and (2) is apparent. The bulk relaxation rate is k_B. In this context, it is completely analogous to a spontaneous rate for quenching of D* (see Sec. II A). Thus we set it to zero in Eq. (43). When an experimental rate is predicted, it will just be a sum of k_B and the rate determined by the solution to this diffusion equation, subject to the boundary conditions, Eq. (44). In the magnetic system, the quenching strength h_{Q_i} (Dh_{Q_i} is sometimes called a "killing strength") depends on the the assumed thickness of the interfacial layer, and details of the atoms involved.

In practical applications, one might measure the total magnetic moment of a sample: $M(t) \equiv \int m(\mathbf{r},t)d\mathbf{r}$, and then attempt to model the solid in order to produce a solution of Eq. (43) which fits $M(t)$. The geometry of the pore walls is an important ingredient, and one might pick a generic shape (slit, cylindrical, or spherical pores, $\cdots$) and then fit other parameters to the data.[36] In order to characterize $M(t)$, one can proceed just as in our original application of diffusion-limited quenching, and extract a pseudo-first-order time, or a mean time, $\bar{\tau}$. In particular, the mean relaxation time has been found to be especially significant in porous solid applications. Torquato[37] has shown that there is a rigorous bound which relates the fluid permeability and the porosity to $\bar{\tau}$ in the limit of strong killing: $h_{Q_i} = \infty$. (This is the diffusion-limited regime.) Wilkinson, Johnson, and Schwartz[34] have extended this bound to finite quenching rates, and have studied $\bar{\tau}$ analytically and numerically for various pore geometries. The notion of reactive enhancement, which occurs when sinks compete for donors may also be applied here, as various pore surfaces compete to relax nuclear spins. This notion is also relevent to spin–spin relaxation. That is, the relaxation rate of N ^{129}Xe atoms within a zeolite pore chamber will be enhanced above N times relaxation rate of one such atom with $N-1$ atoms of the more abundant (spinless) isotope, ^{130}Xe. In Sec. IV, we examine this model in detail.

The notion of reactive enhancement could conceivably increase the difficulty of deducing pore structure from spin–lattice relaxation times, by introducing additional, relevent parameters to the pore model. As an example, consider a slit pore with rough, molecular walls. Suppose that, without altering the wall surfaces or the mean separation, we change the registry between the walls by sliding one along the other. If the walls are far from one another, this shift should have no effect on the rate at which the pore relaxes nuclear spins. If the wall separation is decreased, one may begin to see changes in the relaxation time as the registry changes. To determine when walls are "close enough" to see this effect, one need not only consider the length scale of the surface roughness, but also the length scale $h_{Q_i}^{-1}$. The relative importance of these two length scales depends on the pore model; clearly, the larger $h_{Q_i}^{-1}$, the more the walls will act as independent quenchers, and the less rates will depend on registry.

As a numerical example, we have calculated the pseudo-first-order relaxation rate, k_0, for a two-dimensional model of this type. The pore, which is shown in Figs. 6(a) and 6(b), has five hemispherical bumps along its inner surface. To avoid edge effects in the computation, the pore is assigned periodic boundary conditions in the horizontal direction. Each hemisphere has a radius of 10 units. In Fig. 6(a), the pore walls (sphere centers) are separated by 50 units; in Fig. 6(b) the separation is decreased to 30 units. We have set $h_{Q_i} = \infty$ for the pore surfaces—the strong killing limit. To find k_0, a square grid with spacing of 1 unit was superposed on the space and a solution to Eq. (43) was found by a simple finite-element technique. That is, all grid sites within the pore space begin with a fixed magnetization and the solution to the diffusion equation is generated for successive, discrete time steps. So long as the iteration time is very much less than $1/D$, this method is stable.[38] One can find k_0 either by fitting the long-time decay of $M(t)$ to an exponential, or by using a finite element version of Eq. (25) on $m(\mathbf{r},t)$ at long times; both were done and the results found to be consistent.

The magnetization at a time late in the calculation is shown by the various shadings of grey in the figures.[39] In the top image in Fig. 6(a), the walls are in phase; in the bottom, they are shifted to be 180° out of phase. The magnetization varies swiftly near the walls, but the walls are sufficiently

This article is copyrighted as indicated in the article. Reuse of AIP content is subject to the terms at: http://scitation.aip.org/termsconditions. Downloaded to IP: 130.58.65.20 On: Mon, 09 Feb 2015 20:37:43

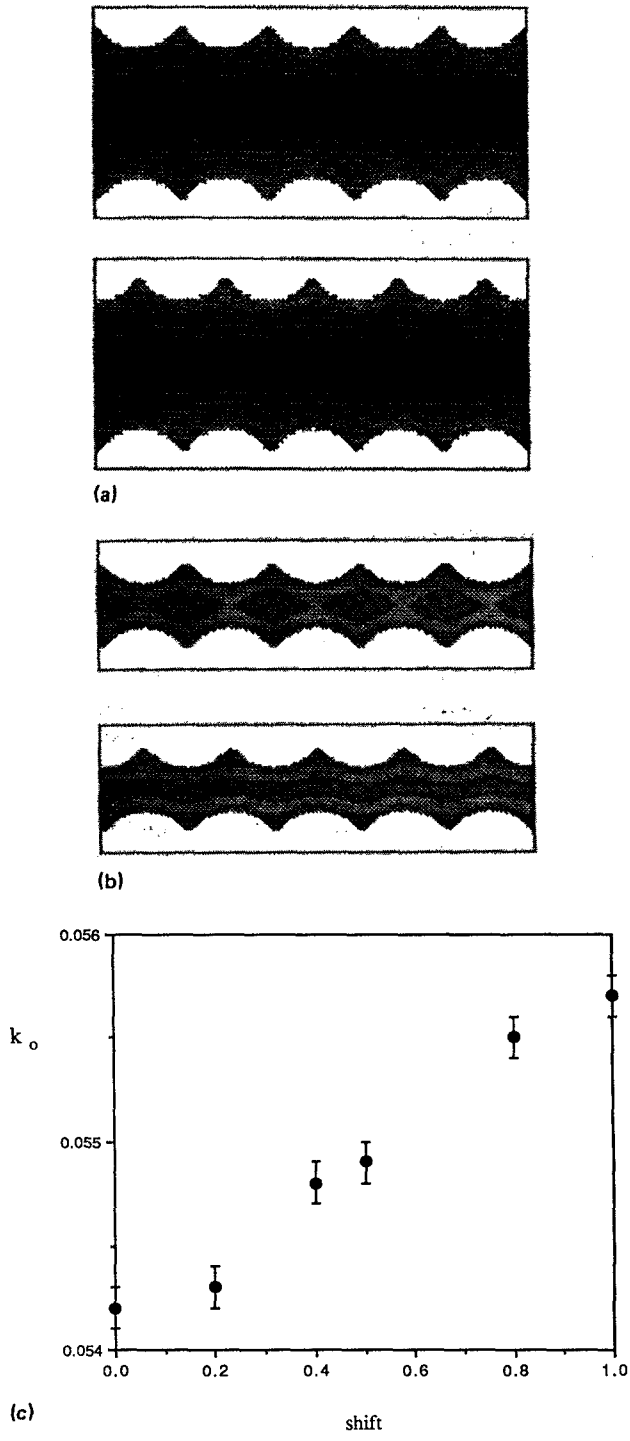


FIG. 6. (a) Two-dimensional model pore. Dimensions are 100 units horizontally, 50 units vertically; grid spacing is 1 unit. White indicates zero magnetization, various grey shades indicate nonzero magnetization. Pore on top has walls in phase; on bottom walls are maximally out of phase. (b) Model as in (a); dimensions are 100 units by 30 units. (c) Pseudo-first-order rate for relaxation of spins as a function of wall shift, in units of sphere radii. One radius = 10 grid spacings.

widely separated that one sees no "communication" between the two walls via the magnetization density. As one expects, when k_0 is calculated for this system, there is no significant change when the walls are shifted. In contrast, when the walls are 30 units apart, as in Fig. 6(b), one sees a real difference in the morphology of the magnetization. The walls compete in a nontrivial way, with the result that k_0 is higher in the maximally shifted system. In fact, for this model the rate rises with shift, as Fig. 6(c) shows. Though k_0 varies by only 3% in this case, this variation will grow as the distance between the walls decreases.

IV. NUMERICAL SIMULATION OF MULTIPLE SINKS

The rate of reaction within a spherical cavity for the single, fixed, central sink can be described analytically as in Sec. II. To examine a quenching reaction in the experimentally interesting case of multiple sinks dispersed within a micelle, we resort to computer simulation. Metropolis MC has long proven useful for such diffusion-reaction problems,[27,40] and has been used for the analagous NMR problem[35] as well. Because reaction is confined to the small, micellar volume, we do not need to resort to certain time-saving techniques[41] which are useful for large systems. Along the lines of our study, Gossele *et al.*[42] and Gratzel[43] have simulated diffusion reaction in micelles. Both studies treat a single pair of reactants in the cavity. The former shows $P(t)$ and compares k_0 to theory and to the rate in homogeneous solutions. The latter compares with experimental data on a triplet–triplet anihilation reaction and, after fitting D from the experimental rate, derives a good estimate of the microviscosity within a micelle.

We model the reaction $D^* + A \rightarrow D + A$ within a cavity 40 Å in diameter. The cavity encloses ten spheres which represent quenching molecules in Cases C and CS, and which serve merely as nonquenching obstacles to the motion of D* in Case S. D* molecules are also modeled as spheres; both D* and A have diameters of 5.0 Å. Then, the volume fraction which excludes D* is greater than or equal to 0.156. (Since D* molecules are not points, the excluded volume depends on the configuration of sinks: their proximity to one another and to the cavity wall.) We study the limit of dilute D*, though our program advances many, noninteracting D* molecules at once for computational efficiency. The A particles are initially distributed at random (but without overlap) throughout the cavity. D* particles begin at locations uniformly distributed outside of the excluded volume, and walk through the cavity with steps of constant length, δ, and random direction. When a walker representing D* encounters an A sphere in Cases C or CS, it is removed from the simulation; it is reflected in Case S. When a walker crosses the micellar surface, it is either removed with probability p, or replaced with probability $1-p$ at its former position. This rule implements the boundary condition, Eq. (2). The value of p must insure that walkers disappear at a rate, R_S say, which is equal to the flux of walkers out through the spherical surface. To find the relationship between p and quenching strength, h_S, imagine that walkers, initially distributed with spherical symmetry, travel in an empty spherical cavity of radius R. Then

$$R_S = D \frac{\partial C(R,t)}{\partial r} 4\pi R^2. \tag{45}$$

This article is copyrighted as indicated in the article. Reuse of AIP content is subject to the terms at: http://scitation.aip.org/termsconditions. Downloaded to IP: 130.58.65.20 On: Mon, 09 Feb 2015 20:37:43

Now consider the number of walkers, $N(R,t)$, which are within a step length, δ, of the surface

$$N(R,t) = C(R,t)4\pi R^2\delta. \tag{46}$$

With this definition, Eqs. (2) and (45) imply

$$R_S \equiv Dh_S N(R,t)/\delta. \tag{47}$$

Consider the random walk simulation. On a single MC step, the number of walkers that will attempt to cross the wall is $\frac{1}{4}N(R,t)$.[44] If the time between walker steps is $\Delta\tau$, which is imagined to be small, then

$$pN(R,t)/4 \equiv R_S\Delta\tau. \tag{48}$$

Using the relationship between a random walk and diffusion in three dimensions: $D = \delta^2/6\Delta\tau$, we arrive at the relationship between p and h_S

$$p = \frac{4R_S\delta^2}{6DN(R,t)} = \frac{2}{3}h_S\delta. \tag{49}$$

This relationship was used with success, for $h_S = 0.5, 0.8$, to test Eqs. (39) and (40) for the total reaction rate in these analytically solvable cases.

Since this problem does not naturally lend itself to a walk on a lattice, this technique was not used. However, though the need to resolve tiny channels between spheres is not as critical as in applications to continuum percolation theory, it is still important to understand whether finite-step-length errors exist. In his on-lattice simulation,[27] Richards varied the ratio of sphere radius to lattice constant from three to six, and then extrapolated the calculated rates to an infinite ratio. This was done for a single volume fraction of 1/3; most data was taken with this ratio at five. Gosele *et al.*[42] also used a grid which was finer than radii of interest. Our Fig. 7 shows k_0 and k as calculated with various step lengths, δ, between 0.75 and 0.15 Å. Since δ determines the diffusion constant and rates are proportional to D, each rate was renormalized to agree upon a D as defined by the 0.25 Å data. Figure 7 shows that, for a single, representative configuration of sinks, neither the mean nor pseudo-first-order rate shows a strong trend with δ in this range.

Computational details are as follows: $N = 800$ walkers were present initially, and the surviving number recorded at each time step. This number divided by N is $P(t)$. Two different cases were studied: one in which A spheres were static and one in which A spheres diffused, with steps which were also of length δ. We chose $\delta = 0.25$ Å. In the case of moving A spheres, a D* sphere was removed from the system in Cases C and CS if it overlapped with an A, no matter whether a move of D* or of A had produced the overlap. In Case S, where the A do not absorb the D* walkers, a move by an A which attempted to superpose two A's was rejected, as was a move by D* which produced overlap with an A. Because we wish to work in the dilute D* limit, yet there are a large number of (noninteracting) D* molecules in the simulation, a move of an A that produced overlap with a D* forced the D* (not the A) to adjust its position in increments of δ until the overlap was removed. In order to find k, one simply sums $P(t)$ until the last walker has disappeared [Eq. (8)]. In order to find k_0, one must fit $P(t)$ to a single exponential at late times. Originally, we divided the data into

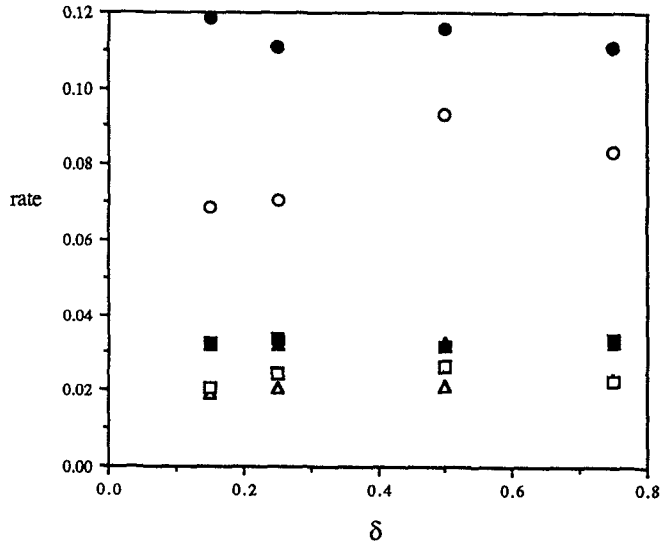


FIG. 7. Pseudo-first-order and mean rates for Cases C, S, and CS in micelle of diameter 40 Å with ten static quenchers of diameter 5.0 Å and single donor of same diameter. Rates are shown as a function of δ, the MC step size, in units of Å. Empty symbols: triangles: k_0^C, squares: k_0^S, circles: k_0^{CS}. Filled symbols: triangles: k^C, squares: k^S, circles: k^{CS}.

blocks by fitting 50 values of $P(t)$ to find k_0, then shifting the time origin by ten steps and fitting the next 50 values to find the next estimate of k_0. There must be (i) no significant trend in the k_0's, and (ii) the standard deviation in the mean must be a small fraction of the mean, in order to identify this mean over many blocks with the pseudo-first-order rate.

A problem with this method was that, at times late enough to show first-order kinetics, the walker number had decreased to the point where statistics were poor. [With less than around 100 walkers in the micelle, one had a noisy estimate of $P(t)$]. To fix this problem, we completed each run in two stages. First, the particle number was allowed to decay to one-tenth (80) of its original value. Then, we replaced every remaining particle with ten new particles at that particle's location, thereby returning to the original concentration, but in a configuration already shaped by the boundary conditions. This "population explosion," in the spirit of a staging calculation, enhanced our ability to resolve the pseudo-first-order rate. The block averaging was done only during the second stage of the calculation, and only while the particle number remained above 400. Each particle in the second stage was given a weight of 1/10 in its contribution to $P(t)$ for the purpose of finding k. We checked that the staging did not bias the measured value of k_0 or k, by comparing with a run in which a much larger original population was allowed to decay with no population explosion. The two sets of results were consistent. Figure 8 shows $\ln P(t)$ vs t for Cases C and CS for a single, static configuration of A molecules. The plotted lines have slopes with values of k_0 given by the block fitting procedure described above; arrows indicate the time at which the walker population explodes. This plot shows that calculated k_0's fit the data well, and that the first stage of the calculation blends smoothly into the second, in terms of the shape of $P(t)$.

This article is copyrighted as indicated in the article. Reuse of AIP content is subject to the terms at: http://scitation.aip.org/termsconditions. Downloaded to IP: 130.58.65.20 On: Mon, 09 Feb 2015 20:37:43

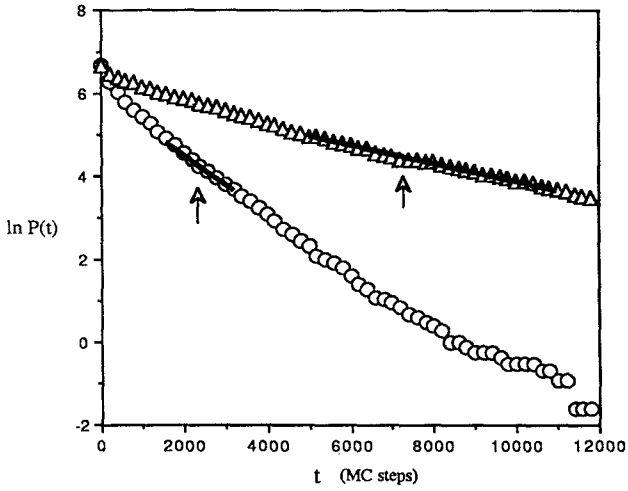


FIG. 8. Natural log of survival probability vs time measured in MC iteration time steps, for micelle with ten static quenchers; $\delta = 0.25$ Å. Triangles: Case C, circles: Case CS. Arrows show time at which population "explodes" to original value. Bold lines have slope of k_0, best-fit as mean from successive blocks of data (see the text). Fitting begins at time shown by arrow; line is extended to show consistency of k_0 before and after explosion.

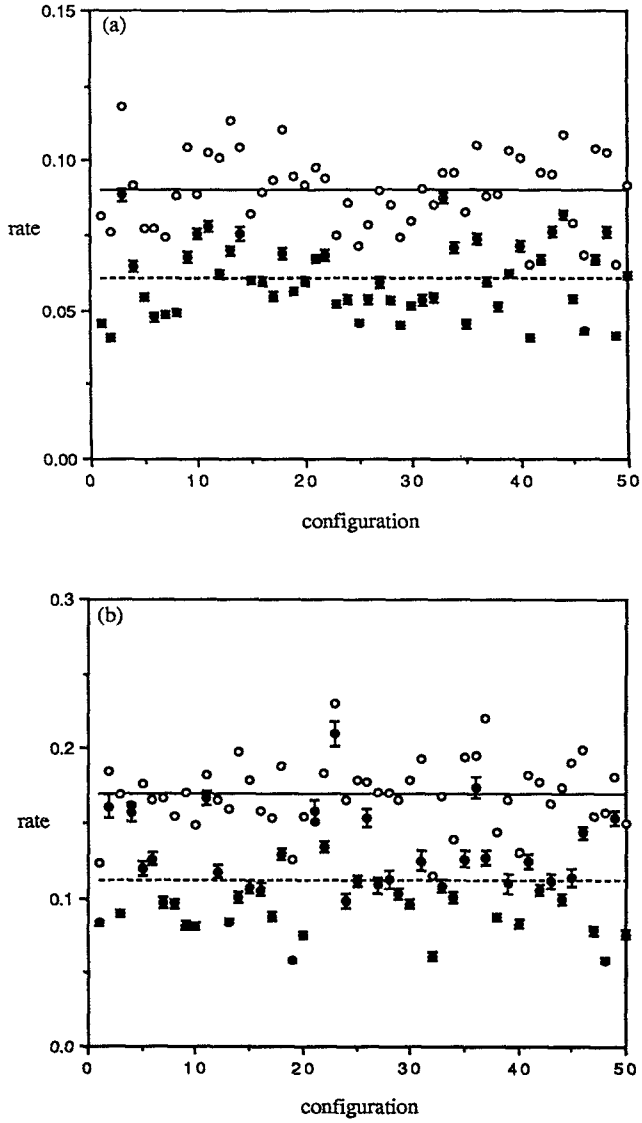


FIG. 9. (a) Pseudo-first-order and mean rates for 50 initial configurations of static quenchers in micellar cavity. Filled circles: k_0, empty circles: k. Dashed line: average k_0, Solid line: average k. (b) Symbols in (a), for moving quenchers.

Finally, we averaged rates over configurational disorder by repeating the calculation for 50 different initial configurations of A molecules. In the case of static A molecules, $h_S = 0.84$ Å^{-1} was chosen. This value gave us a branching ratio (Sec. II B) of roughly unity; the mean over configurations was $B = 1.1$. (All uncertainties are one unit in last decimal place unless otherwise noted.) Figure 9(a) shows raw data for Case CS. Error bars on k_0 arise from the block averaging procedure for a single configuration. The dispersion in the average of k_0 over configurations is clearly dominated by fluctuations in k_0 from one configuration to another, rather than the error in k_0 for a single configuration; this is as one would hope. Figure 9(b) shows raw data for Case CS in the case of moving A molecules. If these molecules had the time, during the course of the simulation, to explore the micelle thoroughly, we would see the scatter in the data of Fig. 9(b) decrease dramatically over that of Fig. 9(a). In fact we do not—at this high volume fraction of quenchers, with donors and quenchers of equal radii, the reaction proceeds quickly on the time scale for quencher motion.

If no other parameter of the simulation is changed, reaction rates roughly double from the static to the moving A case. This is because the effective (pair) diffusion constant has doubled. However, if we are interested in finding large relative enhancements δk_0 and δk, we try to adjust parameters so that B remains at or slightly below unity (Sec. II B). When the A are free to move, B rises to around 1.4. The least consequential way to reduce B is to raise the surface quenching strength, h_S. If it is raised to the point that the surface is a perfect quencher, the branching ratio falls to approximately $B = 1.0$. Thus, the data of Fig. 9(b) are taken in this limit.

Table II contains final data; it shows pseudo-first-order and mean rates for schemes C, S, and CS for the cases of static and moving quenchers.[45] It also shows the absolute and relative enhancements of the rates. For all cases in the table, for moving as well as static quenchers, mean rates exceed pseudo-first-order rates. The excess is from 15%–35% of the mean rate. The disagreement between k and k_0 implies that pseudo-first-order kinetics are not quickly established here. Thus we would not want to characterize the reactor entirely by k_0, as some previous workers have done. For this reactive geometry in the case of static quenchers, there cannot be a good separation of eigenvalues of Eq. (4). This is reasonable for Cases S and CS because h_S is far from zero—and is true also in Case C where the surface quenching strength vanishes. The relative enhancements, δk_0 and δk, are large. One cannot construct a central sink model with enhancements of this magnitude for the same surface

This article is copyrighted as indicated in the article. Reuse of AIP content is subject to the terms at: http://scitation.aip.org/termsconditions. Downloaded to IP: 130.58.65.20 On: Mon, 09 Feb 2015 20:37:43

TABLE II. Rates, absolute (Δ rate), and relative (δ rate) enhancements for reaction in a 40 Å micelle with 10, 5.0 Å static ($h_S = 0.84\,\text{Å}^{-1}$) and moving ($h_S = \infty$) quenchers. Rates are renormalized so that $D \equiv 1.0\,\text{Å}^2/\text{ps}$.

	C	S	CS	Δ Rate	δ Rate
			Static		
k_0	0.017 ± 0.001	0.0223 ± 0.0004	0.060 ± 0.002	0.021 ± 0.002	35%
k	0.026 ± 0.001	0.0319 ± 0.0004	0.090 ± 0.002	0.032 ± 0.002	36%
			Moving		
k_0	0.045 ± 0.003	0.034 ± 0.001	0.111 ± 0.005	0.032 ± 0.006	29%
k	0.056 ± 0.002	0.0504 ± 0.0005	0.169 ± 0.003	0.063 ± 0.004	37%

quenching strength. That is, referring back to Figs. 3(c) and 5(c), there is no radius of central sink which, given $h_S = 0.84$, will produce 35% enhancements as seen for the static data in Table II. To summarize a main point: One cannot view reactions at the surface and within this micelle as occuring in parallel. Any analysis of such a system which begins with the assumed superposition of rates, $k^C + k^S = k^{CS}$, will begin with an error which propagates through the calculation. For the (physically motivated) parameters we have studied, this initial error is roughly 35%.

In conclusion, we have studied the absolute and relative enhancement in reaction rate that is achieved by placing quenchers both within and on the surface of a micellar cavity. We have found significant enhancement both in the case of a single, central quencher, and for dispersed static and moving quenchers in a micelle—enhancements not too far below a conjectured maximum of 50%. These results imply that, in general, one cannot view reaction at the surface and within the micellar volume as channels which operate in parallel, save in the limit of weak quenching and small quencher radius. On a more positive note, the results suggest a way to enhance the efficiency of a diffusion-limited reaction within a micelle or porous solid. One attempts to distribute reagent or catalyst simultaneously on surfaces which are expected to compete; just as surfaces within the pore and at the pore surface compete in the present study. Finally, we have noted that these results apply to the relaxation of magnetization as seen through NMR measurements, and have studied a type of competition between relaxing surfaces in a simple model of a pore with rough walls.

We thank J. Boccio, P. Collings, R. Dumont, D. Johnson, and J. Talvaccia for helpful discussions. We are also grateful for computing support from M. Wall and the Academic Computing Center, and we gratefully acknowledge financial support from the Division of Natural Sciences, the Faculty Research Support Fund, and the Provost's office at Swarthmore College. Acknowledgment is made to the donors of the Petroleum Research Fund, administered by the American Chemical Society, for support of this research under Grant No. 19890-AC6. Finally, we gratefully acknowledge grant support of computer time on a CRAY Y-MP from the Academic Affiliates Program at the National Center for Supercomputing Applications at the University of Illinois, Urbana-Champaign.

[1] G. Adam and M. Delbruck, in *Structural Chemistry and Molecular Biology*, edited by A. Rich and N. Davidson (Freeman, San Francisco, 1968).
[2] M. D. Hatlee, J. J. Kozak, G. Rothenberger, P. P. Infelta, and M. Gratzel, J. Phys. Chem. **84**, 1508 (1980).
[3] A. J. Frank, M. Grazel, and J. J. Kozak, J. Am. Chem. Soc. **98**, 3317 (1976); J. H. Fendler, Acc. Chem. Res. **13**, 7 (1980); J. H. Fendler and E. J. Fendler, *Catalysis in Micellar and Macromolecular Systems* (Academic, New York, 1985).
[4] I. R. Gould, M. B. Zimmt, N. J. Turro, B. H. Baretz, and G. F. Lehr, J. Am. Chem. Soc. **107**, 4607 (1985); N. J. Turro, M. B. Zimmt, X. G. Lei, I. R. Gould, K. S. Nitsche, and Y. Cha, J. Phys. Chem. **91**, 4544 (1987).
[5] K. Kalyanasundaram, *Photochemistry in Microheterogeneous Systems* (Academic, New York, 1987).
[6] M. Tachiya, in *Kinetics of Nonhomogeneous Processes*, edited by G. R. Freeman (Wiley, New York, 1987).
[7] J. R. Escabi-Perez, A. Romero, S. Lukac, and J. H. Fendler, J. Am. Chem. Soc. **101**, 2231 (1979); Y. Moroi, A. M. Braun, and M. Gratzel, *ibid.* **101**, 567 (1979).
[8] T. Nomura, J. R. Escabi-Perez, J. Sunamoto, and J. H. Fendler, J. Am. Chem. Soc. **102**, 1484 (1980).
[9] V. Ramesh and M. M. Labes, J. Am. Chem. Soc. **108**, 4643 (1986); V. Ramesh and M. M. Labes, Mol. Cryst. Liq. Cryst. **144**, 257 (1987).
[10] M. Almgren, J. Alsins, E. Mukhtar, and J. van Stam, J. Phys. Chem. **92**, 4479 (1988).
[11] R. Aris, *The Mathematical Theory of Diffusion and Reaction in Permeable Catalysis*, Vols. I and II (Clarendon, Oxford, 1975).
[12] R. Samson and J. M. Deutch, J. Chem. Phys. **68**, 285 (1978).
[13] M. Van der Auweraer, J. C. Dederen, E. Gelade, and F. C. De Schryver, J. Chem. Phys. **74**, 1142 (1981).
[14] See the "ink-bottle" pore model of Chu and Chon in Chap. 3 of Ref. 11.
[15] H. S. Carslaw and J. C. Jaeger, *Conduction of Heat in Solids* (Oxford University, London, 1959); E. F. Casassa and Y. Tagami, Macromolecules **2**, 14 (1969); M. Tachiya, Chem. Phys. Lett. **69**, 605 (1980).
[16] H. Sano and M. Tachiya, J. Chem. Phys. **75**, 2870 (1981).
[17] P. P. Infelta, M. Gretzel, and J. K. Thomas, J. Phys. Chem. **78**, 190 (1974); J. C. Dederen, M. Van der Auweraer, and F. C. De Schryver, Chem. Phys. Lett. **68**, 451 (1979); P. P. Infelta and M. Gratzel, J. Chem. Phys. **70**, 179 (1979).
[18] M. Tachiya, Chem. Phys. Lett. **33**, 289 (1975); P. P. Infelta and M. Gratzel, J. Chem. Phys. **78**, 5280 (1983); M. Tachiya, *ibid.* **78**, 5282 (1983).
[19] M. D. Hatlee and J. J. Kozak, J. Chem. Phys. **72**, 4358 (1980).
[20] For a review, see G. H. Weiss, J. Stat. Phys. **42**, 3 (1986); more recently, K. Mattern and B. U. Felderhof, Physica A **143**, 1 (1987); J. Rubinstein and S. Torquato, J. Chem. Phys. **88**, 6372 (1988); M. Lowenberg and G. R. Gavalas, J. Chem. Phys. **90**, 177 (1989).
[21] C. W. J. Beenakker and J. Ross, J. Chem. Phys. **84**, 3857 (1986); K. Mattern and B. U. Felderhof, *ibid.* **85**, 5382 (1986); also see Ref. 27.
[22] M. Smoluchowski, Phys. Z. **17**, 557 (1916).
[23] P. M. Richards, J. Chem. Phys. **85**, 3520 (1986).
[24] R. I. Cukier, J. Stat. Phys. **42**, 69 (1986).
[25] A. Stern and M. Volmer, Phys. Z. **20**, 183 (1919).
[26] G. Arfken, *Mathematical Methods for Physicists* (Academic, New York, 1985).
[27] P. M. Richards, Phys. Rev. B **35**, 248 (1987).

This article is copyrighted as indicated in the article. Reuse of AIP content is subject to the terms at: http://scitation.aip.org/termsconditions. Downloaded to IP: 130.58.65.20 On: Mon, 09 Feb 2015 20:37:43

[28] U. Gosele and A. Seeger, Philos. Mag. **34**, 177 (1976).
[29] G. H. Weiss, Adv. Chem. Phys. **13**, 1 (1967).
[30] A. Szabo, K. Schulten, and Z. Schulten, J. Chem. Phys. **72**, 4350 (1980).
[31] J. Rauch, in *Lecture Notes in Mathematics*, **446**, edited by J. A. Goldstein (Springer, Berlin, 1975).
[32] W. E. Kenyon, P. Day, C. Straley, and J. Willemsen, paper SPE-15643, presented at 61st Annual Technical Conference of Society of Petroleum Engineers, New Orleans, 1986; C. Straley, A. Matteson, S. Feng, L. M. Schwartz, W. E. Kenyon, and J. R. Banavar, Appl. Phys. Lett. **51**, 1146 (1987); J. Fraissard and T. Ito, Zeolites **8**, 350 (1988).
[33] J. A. Ripmeester and D. W. Davidson, J. Mol. Struct. **75**, 67 (1981).
[34] D. J. Wilkinson, D. L. Johnson, and L. M. Schwartz, Phys. Rev. B **44** II, 4960 (1991).
[35] J. R. Banavar and L. M. Schwartz, Phys. Rev. Lett. **58**, 1411 (1987).
[36] K. R. Brownstein and C. E. Tarr, Phys. Rev. A **19**, 2446 (1979).
[37] S. Torquato, Phys. Rev. Lett. **64**, 2644 (1990).
[38] C. R. Wylie and L. C. Barrett, *Advanced Engineering Mathematics* (McGraw-Hill, New York, 1982), Chap. 5.
[39] Figure 6 uses a "high frequency" palette, in which the darkness of grey shading tends to increase as density increases, but with an oscillatory character.
[40] M. Dumont, J. Ravez, and P. M. Petropoulos, in *Proceedings of 2nd European Simulation Congress*, edited by G. C. Vansteenkiste (Antwerp, 1986).
[41] L. H. Zheng and Y. C. Chiew, J. Chem. Phys. **90**, 322 (1989).
[42] U. Gosele, U. K. A. Klein, and M. Hauser, Chem. Phys. Lett. **68**, 291 (1979).
[43] M. Gratzel, Tetrahedron **43**, 1679 (1987).
[44] We assume that δ is sufficiently small so that (i) The curvature of the shell of width δ can be neglected on the scale of the walker's motion: $\delta \ll R$; (ii) The concentration is roughly uniform in the shell. With these two assumptions, one calculates the likelihood that a walker a distance $z \lesssim \delta$ from the wall crosses it on the next step, and then averages over all z between 0 and δ, to find a factor of 1/4.
[45] Since there is no time interval associated, a priori, with one MC iteration time, we can assign $\Delta\tau$ a value (of 0.010 ps) so that for $\delta = .25$ Å, particles move as if they were diffusing in three dimensions with $D = 1.0$ Å^2/ps. The reported values in Table II reflect this choice.

This article is copyrighted as indicated in the article. Reuse of AIP content is subject to the terms at: http://scitation.aip.org/termsconditions. Downloaded to IP: 130.58.65.20 On: Mon, 09 Feb 2015 20:37:43